Uneven balance of power between hypothalamic peptidergic neurons in the control of feeding

Qiang Wei[a], David M. Krolewski[a], Shannon Moore[a], Vivek Kumar[a], Fei Li[a], Brian Martin[a], Raju Tomer[b], Geoffrey G. Murphy[a], Karl Deisseroth[c], Stanley J. Watson Jr.[a], and Huda Akil[a,1]

[a]Molecular and Behavioral Neuroscience Institute, University of Michigan, Ann Arbor, MI 48109; [b]Department of Biological Sciences, Columbia University, New York, NY 10027; and [c]Department of Bioengineering, Stanford University, Stanford, CA 94305

Contributed by Huda Akil, August 7, 2018 (sent for review February 6, 2018; reviewed by Olivier Civelli and Allen Stuart Levine)

Two classes of peptide-producing neurons in the arcuate nucleus (Arc) of the hypothalamus are known to exert opposing actions on feeding: the anorexigenic neurons that express proopiomelanocortin (POMC) and the orexigenic neurons that express agouti-related protein (AgRP) and neuropeptide Y (NPY). These neurons are thought to arise from a common embryonic progenitor, but our anatomical and functional understanding of the interplay of these two peptidergic systems that contribute to the control of feeding remains incomplete. The present study uses a combination of optogenetic stimulation with viral and transgenic approaches, coupled with neural activity mapping and brain transparency visualization to demonstrate the following: (*i*) selective activation of Arc POMC neurons inhibits food consumption rapidly in unsated animals; (*ii*) activation of Arc neurons arising from POMC-expressing progenitors, including POMC and a subset of AgRP neurons, triggers robust feeding behavior, even in the face of satiety signals from POMC neurons; (*iii*) the opposing effects on food intake are associated with distinct neuronal projection and activation patterns of adult hypothalamic POMC neurons versus Arc neurons derived from POMC-expressing lineages; and (*iv*) the increased food intake following the activation of orexigenic neurons derived from POMC-expressing progenitors engages an extensive neural network that involves the endogenous opioid system. Together, these findings shed further light on the dynamic balance between two peptidergic systems in the moment-to-moment regulation of feeding behavior.

proopiomelanocortin | agouti-related protein | feeding | arcuate nucleus | satiety

Global epidemic obesity underscores the critical need for understanding how the brain regulates food intake (1). Feeding is essential for survival and relies on mechanisms that monitor energy demands and metabolic status. But feeding behavior is more complex, as it has a strong rewarding component (2) and can respond to environmental stimuli, including stress and social context (3). Therefore, it is critical to unravel the mechanisms that modulate both the initiation and the cessation of feeding.

It is well established that the hypothalamus plays an essential role in the regulation of feeding behavior and contributes to the process of energy homeostasis (4, 5). Hypothalamic nuclei engaged in this regulation include the Arc, the paraventricular nucleus (PVN), the lateral hypothalamic (LH) area, the dorsomedial nucleus, and the ventromedial nucleus. Disruption of the ventromedial hypothalamus induces hyperphagia and obesity, while disruption of the lateral hypothalamus causes hypophagia and weight loss, suggesting the existence of ventromedial "satiety" and lateral "feeding" centers (6). Recent work has extended these early observations and has focused on the Arc of the hypothalamus, a nucleus particularly important for the central regulation of appetite, energy expenditure, and body weight (7, 8).

Two classes of peptide-producing neuronal populations in the Arc play a central and antagonistic role in the control of appetite—the orexigenic neurons that express AgRP and NPY promote food consumption, while anorexigenic neurons that express POMC inhibit feeding behavior. AgRP/NPY neurons are active when the energy stores are not sufficient to meet systemic demands, thereby releasing AgRP and promoting feeding (9, 10). POMC is a complex polypeptide precursor cleaved into active peptides including melanocortins and β-endorphin (11). While β-endorphin is a long-acting opioid analgesic (12), the cosynthesized α-melanocyte stimulating hormone (α-MSH) blocks appetite (13). These two sets of peptidergic neurons in the Arc respond to nutrient and hormonal signals from the periphery. Thus, leptin, a signal of positive energy balance, stimulates POMC neurons, leading to decreased food intake while inhibiting the release of the orexigenic peptides from neighboring AgRP/NPY neurons (10). Together, AgRP/NPY neurons and POMC neurons work coordinately to integrate signals of energy homeostasis and to regulate feeding behavior (8, 14).

Evidence suggests that these two peptidergic systems that control feeding emerge from a common cellular origin. A developmental study has demonstrated that embryonic POMC-expressing progenitors not only give rise to adult POMC cells, but also differentiate into non-POMC neurons, including NPY neurons (15). This means transgenic studies that target POMC cells in early development can capture both adult populations, whereas adult delivery of viral vectors can target POMC cells selectively. Consequently, we used optogenetic stimulation relying on both virally mediated and traditional transgenic approaches to deliver blue light-activated channelrhodopsin 2 (ChR2) to POMC neurons in the Arc. We coupled this stimulation with behavioral assessments and anatomical analyses examining the

Significance

The interplay between the anorexigenic and orexigenic neurons in the arcuate nucleus that contributes to the control of feeding remains elusive. Using optogenetic stimulation, we show that activation of POMC neurons rapidly inhibits feeding behavior in fasted animals. However, simultaneous stimulation of both POMC neurons and a subset of the orexigenic neurons that express AgRP is sufficient to reverse that inhibition and trigger intense feeding behavior. We used 3D imaging and functional studies to illuminate the anatomical underpinning of both the inhibitory and excitatory events. Our work suggests that translational applications that aim to control appetite need to target the activation rather than the inhibition mechanisms.

Author contributions: Q.W., R.T., G.G.M., K.D., S.J.W., and H.A. designed research; Q.W., D.M.K., S.M., V.K., F.L., and B.M. performed research; Q.W., D.M.K., S.M., V.K., and B.M. analyzed data; and Q.W. and H.A. wrote the paper.

Reviewers: O.C., University of California, Irvine; and A.S.L., University of Minnesota.

The authors declare no conflict of interest.

[1]To whom correspondence should be addressed. Email: akil@umich.edu.

This article contains supporting information online at www.pnas.org/lookup/suppl/doi:10.1073/pnas.1802237115/-/DCSupplemental.

Published online September 17, 2018.

extent of activation and its consequences on cFos expression throughout the brain. Thus, we selectively activated neurons derived from POMC-expressing progenitors in the Arc and ascertained the net impact on food intake in adult mice. We contrasted the effect of activating only the POMC neurons versus the impact of activating both POMC and AgRP/NPY neurons simultaneously on food consumption in mice. Our findings indicate that selective activation of Arc POMC neurons inhibits food consumption rapidly in fasted animals whereas activation of Arc neurons arising from POMC-expressing progenitors results in a robust increase in food intake. We show that in the conflict between the drive to consume food and the rapid satiety control that inhibits feeding, the former dominates, resulting in an acute increase in feeding. These opposing effects are associated with distinct projection and activation patterns. Thus, the regulation of feeding behavior involves a dynamic balance between the two peptidergic systems.

Results

Characterization of Viral POMC-ChR2 Mice. To control hypothalamic POMC neurons selectively, we used a Cre-dependent adeno-associated virus (AAV) vector carrying the gene encoding the blue light-activated cation channel ChR2 fused to enhanced yellow fluorescent protein (eYFP). This Cre-inducible double-floxed inverted ORF (DIO) AAV viral vector AAV5-EF1α-DIO-ChR2(H134R)-eYFP (Fig. 1*A*) was microinjected into the Arc of adult POMC-Cre transgenic mice (16). Upon transduction, Cre-expressing POMC neurons invert the ChR2-eYFP ORF in irreversible means and ChR2-eYFP proteins are expressed under control of the elongation factor 1α promoter (referred to as viral POMC-ChR2). This approach allowed us to selectively stimulate Arc POMC neurons with blue light (473 nm). We validated the cell-type selectivity of this viral approach in coronal Arc sections of viral POMC-ChR2 mice. ChR2-eYFP specifically colocalized with endogenous POMC neurons (Fig. 1*B*). On average, 80% of POMC-positive neurons were positive for ChR2-eYFP in the virus injection sites (Fig. 1*C*). Of the ChR2-eYFP expressing cells, 93% were colocalized by POMC immunostaining (Fig. 1*C*), demonstrating high specificity of ChR2 expression in the POMC neurons of the Arc of the viral POMC-ChR2 mice. To confirm the functional impact of ChR2 activation in the viral POMC-ChR2 mice, the Arc was illuminated with blue light while the animal explored an open field chamber. Expression of the neuronal activity marker, immediate early gene cFos, was evaluated in the Arc of the viral POMC-ChR2 mice with or without optic stimulation. Activity in the region of virus injection was increased by approximately sevenfold following blue light stimulation [cFos-positive neurons per section: laser off (n = 3 mice), 6.14 ± 1.27; laser on (n = 5 mice), 40.80 ± 3.74; unpaired two-tailed t test, $t(6) = 6.83$, $P < 0.01$]. Of cFos-positive cells, 77% were

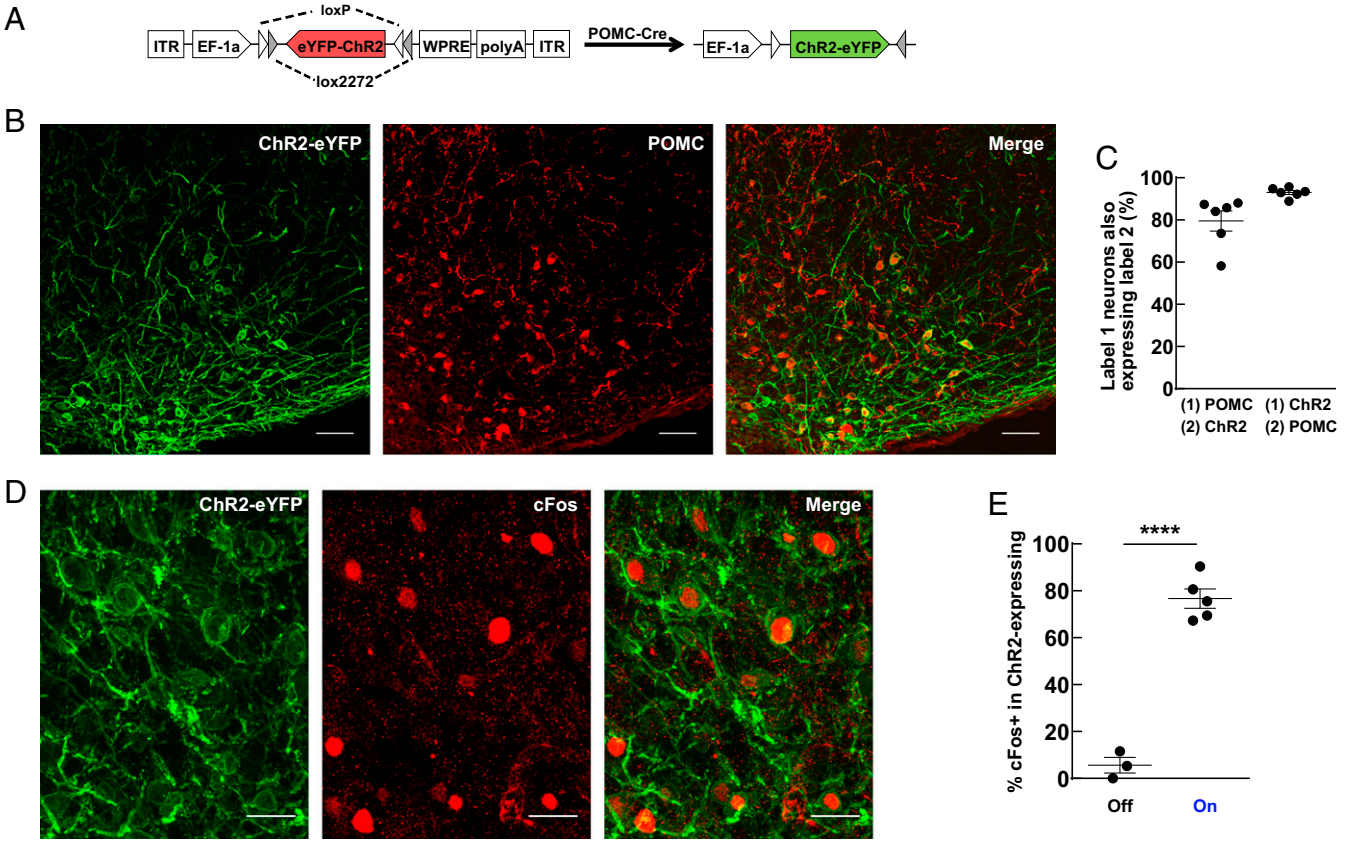

Fig. 1. Characterization of viral POMC-ChR2 mice. (*A*) Schematic of the Cre-dependent AAV. The ChR2-eYFP gene is doubly flanked by two sets of incompatible lox sites. Upon delivery into POMC-Cre transgenic mouse line, ChR2-eYFP is inverted to enable transcription from the EF-1α promoter. (*B*) Representative images showing cell-specific ChR2-eYFP expression (green) in POMC neurons (red) in the Arc of the hypothalamus. (Scale bar, 50 μm.) (*C*) Statistics of expression in POMC neurons (n = 6 mice, 894 POMC neurons, 738 ChR2-eYFP neurons). Eighty percent of POMC neurons expressed in ChR2-eYFP neurons; 93% of ChR2-eYFP neurons expressed in POMC neurons. Mean ± SEM. (*D*) Blue light illumination of the Arc led to induction of cFos (red) in ChR2-eYFP-positive neurons (green). (Scale bar, 20 μm.) (*E*) Statistics of cFos-positive neurons in ChR2-eYFP expressing cells at implant region of the Arc with or without optic stimulation. Six percent of cFos-positive neurons expressed in ChR2-eYFP neurons in the no-optic stimulation group (n = 3 mice, 55 cFos-positive neurons, 410 ChR2-eYFP neurons) versus 77% in light-stimulation group (n = 5 mice, 538 cFos-positive neurons, 554 ChR2-eYFP neurons). Unpaired two-tailed t test: $t(6) = 11.77$, ****$P < 0.0001$. Mean ± SEM.

colabeled by ChR2-eYFP staining (Fig. 1 *D* and *E*). In contrast, 6% of cFos-positive cells were colocalized in ChR2-eYFP staining in the no-stimulation group (Fig. 1*E*). These results indicate selective and effective local activation of POMC neurons in the viral POMC-ChR2 mice.

Characterization of Transgenic POMC-ChR2 Mice. To target ChR2 expression selectively in POMC progenitors, the POMC-Cre mouse line was crossed to a conditional mouse line containing Rosa26-CAG-stop^{flox}-ChR2(H134R)-eYFP (17). Offspring of the double transgenic mouse line are hereafter referred to as transgenic POMC-ChR2 (Tg POMC-ChR2) (Fig. 2*A*). Adult Tg POMC-ChR2 mice exhibited robust expression of ChR2-eYFP in the Arc (Fig. 2*B*). We found that both POMC-positive (Fig. 2*C*) and AgRP-positive (Fig. 2*D*) neurons were detected in ChR2-eYFP expressing cells, indicating that the POMC-expressing lineage gives rise to two opposing neuronal populations in the Arc during development. This is consistent with the view that embryonic POMC-expressing progenitors differentiate into AgRP/NPY expressing cells (15). Furthermore, our immunostaining study revealed that this group of AgRP-positive neurons derived from POMC-expressing progenitors represents a subset of AgRP neurons in the Arc (Fig. 2*D*).

Ex vivo, whole-cell current-clamp recording revealed that ChR2-eYFP-positive cells fired action potentials in response to repeated light-stimulation patterns used in the hot-plate and food intake tests of the current study (Fig. 2 *E* and *F*), indicating that ChR2-expressing cells were capable of responding to light pulses during the entire behavioral testing sessions and they were well tolerant to light stimulations.

Blue light stimulation of the Arc of Tg POMC-ChR2 mice induced a significant increase in cFos expression in the region below the implanted optic fiber [cFos-positive neurons per section: laser off ($n = 3$ mice), 4.06 ± 0.82; laser on ($n = 3$ mice), 49.17 ± 1.12; unpaired two-tailed t test, $t(4) = 32.5$, $P < 0.0001$]. Sixty-one percent of ChR2-eYFP expressing neurons were activated in the light-stimulation group compared with 5% in the group without stimulation (Fig. 2*G*). Using triple-label immunostaining, we found that both POMC-positive and AgRP-positive neurons (Fig. 2 *H* and *I*) were activated by light stimulation as assessed by induction of the cFos. These results demonstrate that, in adult Tg POMC-ChR2 mice, ChR2 proteins are expressed in POMC or AgRP neurons and these two opposing neuronal populations are simultaneously activated by light stimulation.

Rapid Inhibition of Feeding Behavior in Fasted Viral POMC-ChR2 Mice. We first examined whether activating POMC neurons by optogenetic stimulation was sufficient to reduce food intake in viral POMC-ChR2 mice. Food consumption was measured for 30 min each day for three consecutive days (day 1, blue laser off; day 2, blue laser on; day 3, blue laser off). Mice were food-deprived for 4 h each day before the food intake test. The laser stimulation parameters used on day 2 were 15-ms light pulses at 10 Hz for 30 s every minute for 30 min. Stimulation of Arc POMC neurons in fasted viral POMC-ChR2 mice resulted in a significant reduction in food intake (Fig. 3*A*). In addition, we studied the impact on pain regulation since this is one of the most classical and well-established effects of β-endorphin (18). The latency for the mice to lick their paws was measured in the hot-plate test. Viral POMC-ChR2 mice showed an increased nociceptive threshold following light stimulation (Fig. 3*B*). This analgesic effect induced by light stimulation could be blocked by pretreatment with the opioid antagonist naloxone (Fig. 3*C*), suggesting that β-endorphin was released by activation of Arc POMC neurons. Together, these results demonstrate that functional neuropeptides in POMC neurons can be released by light stimulation, and activation of Arc POMC neurons leads to acute inhibition of food intake in fasted animals.

Rapid and Robust Increase in Food Intake in Tg POMC-ChR2 Mice. In Tg POMC-ChR2 mice, ChR2 protein was expressed in neurons derived from POMC-expressing progenitors in the Arc including POMC- and AgRP-positive neurons. We also demonstrated that both POMC and AgRP neurons are simultaneously activated by light stimulation in the Arc of Tg POMC-ChR2 mice. Hot-plate and food intake tests were performed in this double transgenic mouse line. Activation of the Arc in Tg POMC-ChR2 mice by light stimulation induced an acute analgesic effect in the hot-plate test (Fig. 4*A*), which could be blocked by pretreatment with naloxone (Fig. 4*B*). This suggests that POMC neurons in the Tg POMC-ChR2 mice are functionally activated by optogenetic stimulation. Latency for single transgenic littermate control mice without ChR2-eYFP expression to lick their paws was unchanged following optogenetic stimulation (Fig. 4*A*). Surprisingly, Tg POMC-ChR2 mice displayed a vigorous increase in food intake in response to light stimulation in the Arc (Fig. 4*C*). There was no change in food consumption in control mice following photostimulation (Fig. 4*C*). These results demonstrate that activation of the Arc in Tg POMC-ChR2 mice leads to a dramatic increase in food intake, counteracting the effect of activation of POMC neurons in the same area. Thus, the orexigenic neurons that drive food consumption clearly override the anorexigenic neurons that inhibit feeding in this animal model.

Distinct Neuronal Projections Between Viral and Tg POMC-ChR2 Mice Visualized via 3D Imaging. A number of recently developed brain transparency techniques permit the 3D visualization of fluorescent-labeled molecules in genetically modified animals. The CLARITY (19–21) and iDISCO (22) methods are two such approaches capable of illuminating neuronal networks that may offer insight into brain connectivity in large millimeter-thick tissue samples. To better understand the potential association between behavior phenotypes and related brain circuitries, we implemented the CLARITY and iDISCO methods for the viral and Tg POMC-ChR2 animal brain samples, respectively. In the viral POMC-ChR2 mice, anti-GFP antibody-labeled fibers originating from the Arc were observed throughout the extent of analyzed samples (Fig. 5 *A* and *B* and Movies S1 and S2). Our findings show that the Arc POMC neurons send efferent projections to various regions, including: (*i*) ventral to the median eminence; (*ii*) rostral to the medial preoptic nuclei, the bed nucleus of the stria terminalis, the nucleus accumbens (NAcc), the lateral and medial septum, and lateral habenular nucleus; (*iii*) dorsal to the thalamic periventricular nucleus; (*iv*) lateral to the amygdala; (*v*) caudal to the brainstem regions, including the periaqueductal gray; and (*vi*) ventrocaudal to the mammillary nucleus (*SI Appendix*, Table S1). Arc POMC neurons project extensively to paraventricular, dorsomedial, and lateral hypothalamic nuclei. Additionally, anterior and periventricular hypothalamic areas and zona incerta also receive direct and dense inputs from the Arc. Nucleus of the vertical limb of the diagonal and the horizontal limb of the diagonal band also receive direct projections from the Arc POMC neurons (*SI Appendix*, Table S1).

In contrast, in neurons derived from POMC-expressing progenitors in the Arc of the Tg POMC-ChR2 mice, the majority of their projections remain within hypothalamic areas (Fig. 6 *A* and *B* and Movies S3 and S4). Here, anti-GFP antibody-labeled fibers were observed terminating in the paraventricular, periventricular, anterior, and the dorsomedial hypothalamus. It is remarkable that the most qualitatively robust innervation was seen within the lateral hypothalamic nucleus (Fig. 6 *A* and *B* and Movies S3 and S4). We also observed the anti-GFP antibody-labeled signals in the dentate gyrus of the hippocampus (Fig. 6*A*) in Tg POMC-ChR2 mice. This is not surprising, given that expression of POMC follows a dynamic pattern during development and POMC expression in some regions of an embryo is

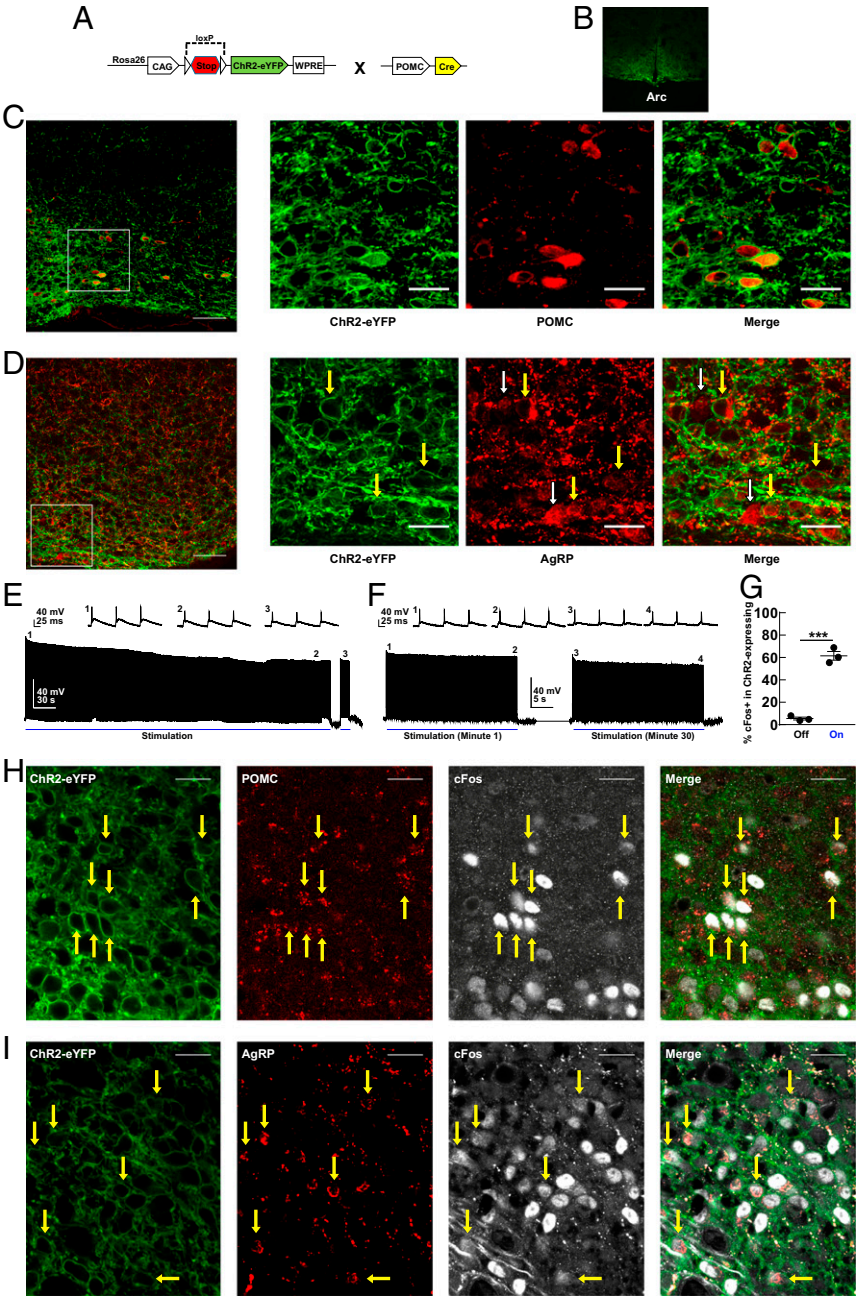

Fig. 2. Characterization of Tg POMC-ChR2 mice. (*A*) Genetic design for ChR2-eYFP expression in the Arc. (*B*) Expression of ChR2-eYFP in the Arc. (*C*) Representative images showing colocalization of POMC-positive neurons with ChR2-eYFP expressing cells in the Arc. *Inset* shows ChR2-eYFP expression (green) in POMC neurons (red). (Scale bar, 50 μm.) (Scale bar in *Inset*, 20 μm.) (*D*) Representative images showing colocalization of AgRP-positive neurons with ChR2-eYFP expressing cells in the Arc. *Inset* shows ChR2-eYFP expression (green) in a subgroup of AgRP neurons (red). Yellow arrows point to ChR2-eYFP-positive AgRP neurons; white arrows point to ChR2-eYFP-negative AgRP neurons. (Scale bar, 50 μm.) (Scale bar in *Inset*, 20 μm.) (*E* and *F*) Representative whole-cell current-clamp recordings of ChR2-eYFP-positive neurons in the Arc from acute slices. To replicate the stimulation pattern used in the hot-plate test, the neuron was stimulated with 15-ms light pulses at 10 Hz for 6 min (indicated by blue bar). After the 6-min period of action potential firing, the light was turned off to show the specificity of the response to light stimulation. Action potential firing resumed at 10 Hz when the light in turned back on. *Insets* show individual action potential firing at 10 Hz at the times indicated by the numbers. To replicate the stimulation pattern used in the food intake study, the neuron was stimulated with 15-ms light pulses at 10 Hz for 30 s (indicated by blue bar) every other 30 s for 30 min. For simplicity, only the first stimulation period (during minute 1; *Left* trace) and the last stimulation period (during minute 30; *Right* trace) are shown. *Insets* show individual action potential firing at 10 Hz at the times indicated by the numbers. $n = 25$ cells, 15 slices from 8 mice. (*G*) Statistics of cFos-positive neurons in ChR2-eYFP expressing cells in the region below the implanted optic fiber in the Arc with or without optic stimulation. Five percent of cFos-positive neurons expressed in ChR2-eYFP neurons in the no-optic stimulation group ($n = 3$ mice, 30 cFos-positive neurons, 522 ChR2-eYFP neurons) versus 61% in the light-stimulation group ($n = 3$ mice, 543 cFos-positive neurons, 901 ChR2-eYFP neurons). Unpaired two-tailed *t* test: $t(4) = 13.63$, $^{***}P < 0.001$. Mean ± SEM. (*H*) Representative images showing the induction of cFos (white) in POMC-positive (red) ChR2-eYFP expressing neurons (green) (yellow arrows) following blue light stimulation in the Arc. POMC-positive neurons were immunostained with anti–β-endorphin antibody. (Scale bar, 20 μm.) (*I*) Representative images showing the induction of cFos (white) in AgRP-positive (red) ChR2-expressing neurons (green) (yellow arrows) following light stimulation in the Arc. (Scale bar, 20 μm.)

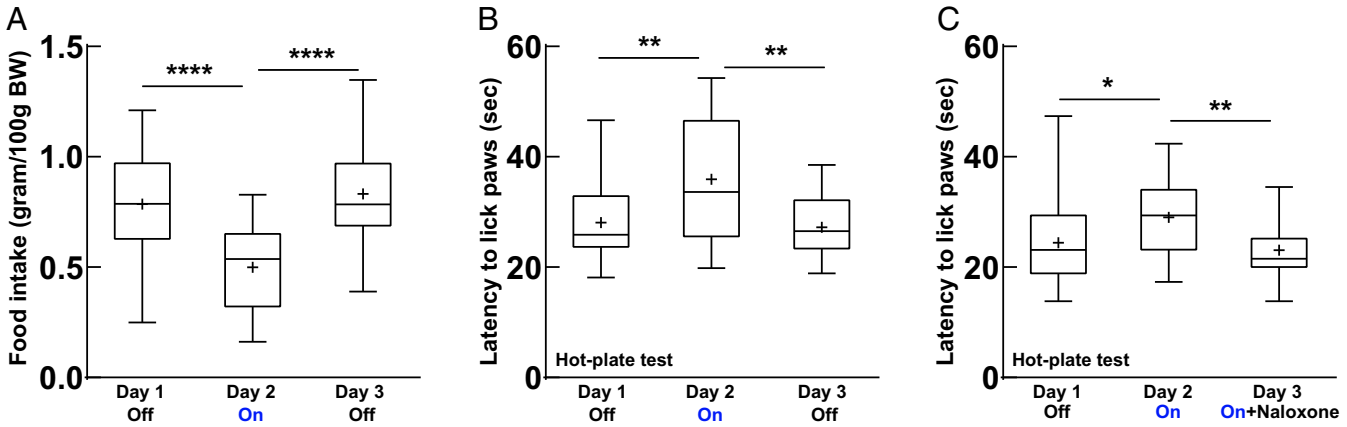

Fig. 3. Selective activation of POMC neurons in the Arc suppresses food intake in fasted viral POMC-ChR2 mice. (*A*) Blue light stimulation of POMC neurons induced a reduction of food intake in 4-h fasted viral POMC-ChR2 mice, $F(2, 40) = 18.99$, $P < 0.0001$; $^{****}P < 0.0001$; $n = 21$ mice. (*B*) Light stimulation of POMC neurons led to an increased latency for the mice to lick their paws during the hot-plate test, $F(2, 30) = 8.82$, $P < 0.01$; $^{**}P < 0.01$; $n = 16$ mice. (*C*) Increased latency induced by light stimulation was blunted by pretreatment with opioid antagonist naloxone (10 mg/kg) in the hot-plate test, $F(2, 28) = 6.797$, $P < 0.01$; $^{*}P < 0.05$; $^{**}P < 0.01$; $n = 15$ mice. Repeated-measures one-way ANOVA followed by Turkey's test were used for all above statistics. Box plots show median, mean (+), lower and upper quartiles (boxes), and minima and maxima (whiskers).

transient (23), including the granule cells of the dentate gyrus (24). These results demonstrate distinct neuronal projection patterns in these two animal models.

Distinct Neuronal Activation Patterns Between Viral and Tg POMC-ChR2 Mice. Given the opposite effects on food intake between viral POMC-ChR2 and Tg POMC-ChR2 mice, we evaluated the neuronal activation as determined by cFos mRNA expression following light stimulation in the Arc in these two animal models. Activation of POMC neurons of the Arc in viral POMC-ChR2 mice led to an increase in cFos in limited brain regions (Fig. 5*C*), including cerebral cortex, lateral septum, PVN, dorsomedial hypothalamus, Arc, and the medial posterior part of the Arc (*SI Appendix*, Table S2). In contrast, activation of the Arc in Tg POMC-ChR2 mice resulted in an intensive cFos response in broader areas of the brain (Fig. 6*C*), including cerebral cortex, prefrontal cortex (PFC), caudate-putamen (CPu), NAcc, septum, lateral thalamus, PVN, LH, dorsomedial hypothalamus, and Arc (*SI Appendix*, Table S3). These results suggest that this acute increase in food intake following activation of the Arc in Tg POMC-ChR2 mice engages an extensive neuronal system in the brain.

Role of Endogenous Opioids in Increased Feeding in Tg POMC-ChR2 Mice. We further investigated the role of endogenous opioids in increased food intake observed in Tg POMC-ChR2 mice. This increased feeding could be largely blocked by pretreatment with naloxone in a dose-dependent manner (Fig. 7*A*), indicating the driving force to consume food can be partially abolished by blocking opioid receptor signaling in this animal model. Following naloxone pretreatment, increased cFos mRNA expression in LH, dorsomedial hypothalamus, and the Arc was observed in response to light stimulation in the Arc of the Tg POMC-ChR2 mice (Fig. 7*B* and *SI Appendix*, Table S4). It should be noted that the induction of neuronal activity in the Arc and LH was reduced by 63% and 52%, respectively, following naloxone pretreatment (Arc: optical density of cFos induction 0.74 versus 0.27 relative to respective control; LH: optical density of cFos

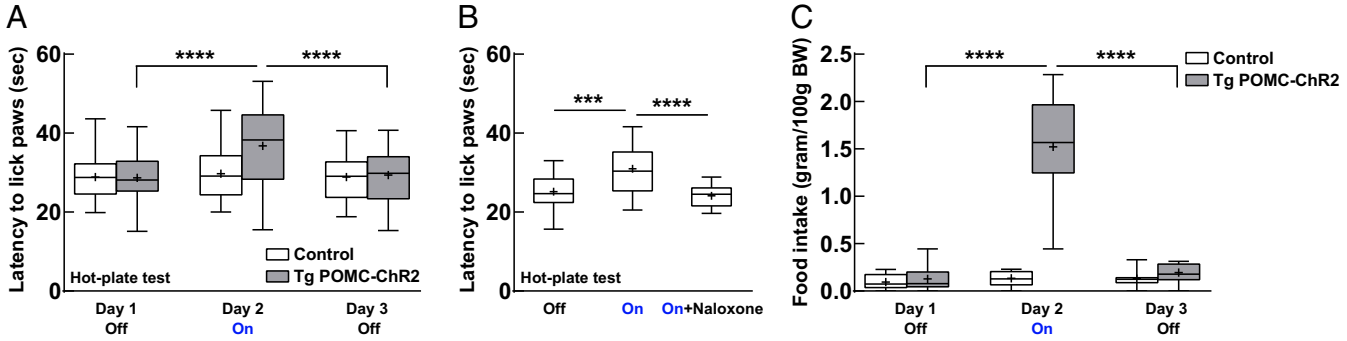

Fig. 4. Activation of Arc neurons derived from POMC-expressing lineage increases food intake in Tg POMC-ChR2 mice. (*A*) Repeated-measures two-way ANOVA revealed a significant genotype × day interaction, $F(2, 82) = 9.44$, $P < 0.001$, for the hot-plate test. Blue light stimulation of Arc neurons in Tg POMC-ChR2 mice led to an increased latency for the animals to lick their paws, $F(2, 52) = 21.91$, $P < 0.0001$; $^{****}P < 0.0001$; $n = 27$ mice. Latency for single transgenic littermate control mice without ChR2-eYFP expression to lick their paws was unchanged, $F(2, 30) = 1.06$, $P = 0.36$; $n = 16$ mice, 8 mice per single transgenic mouse line. (*B*) Increased latency induced by light stimulation in Tg POMC-ChR2 mice was reduced by pretreatment with opioid antagonist naloxone, $F(2, 24) = 15.2$, $P < 0.0001$; $^{***}P < 0.001$, $^{****}P < 0.0001$; $n = 13$ mice. (*C*) Repeated-measures two-way ANOVA revealed a significant genotype × day interaction, $F(2, 54) = 76.59$, $P < 0.0001$, for the food intake study. Light stimulation of Arc neurons evoked a robust increase in food intake in Tg POMC-ChR2 mice, $F(2, 24) = 68.28$, $P < 0.0001$; $^{****}P < 0.0001$; $n = 13$ mice. Food intake for control mice was unchanged following light stimulation of Arc, $F(2, 30) = 1.19$, $P = 0.32$; $n = 16$ mice. Box plots show median, mean (+), lower and upper quartiles (boxes), and minima and maxima (whiskers).

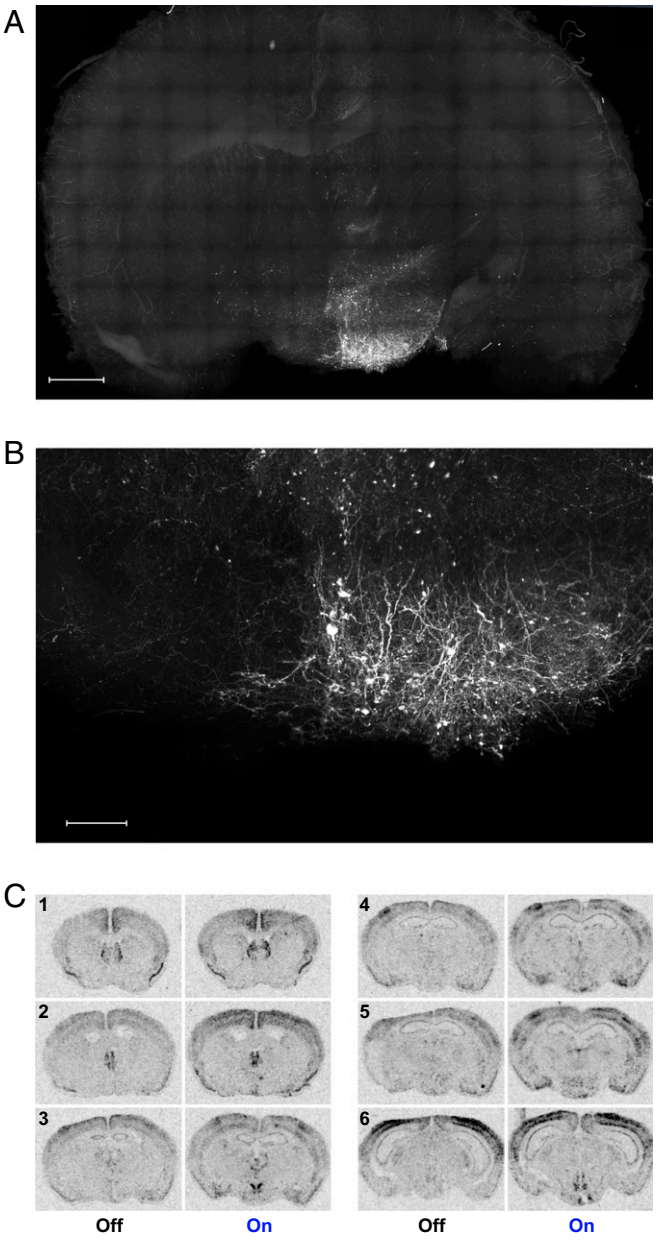

Fig. 5. Anatomical analysis of Arc POMC neuronal projections and the extent of activation in viral POMC-ChR2 mice. (*A*) eYFP-expressing Arc POMC neurons and their connectivity shown as a max intensity z-projection image. Representative CLARITY processed image shows prominent arcuate connectivity with the paraventricular, dorsomedial, and lateral hypothalamus, as well as the zona incerta, periaqueductal gray, and lateral septum in the viral POMC-ChR2 mouse brain slice (4-mm thickness). (Scale bar, 1500 μm.) (*B*) Magnified view shows a more detailed eYFP expression pattern in the Arc in the viral-injected hemisphere. (Scale bar, 600 μm.) (*C*) Neuronal activation in the brain following light stimulation in the Arc of viral POMC-ChR2 mice. ISH revealed cFos mRNA expression was increased in limited brain regions in response to selective activation of Arc POMC neurons. Images were quantitatively analyzed with results shown in *SI Appendix*, Table S2. Representative images are shown ranging from Bregma 1.10 mm (indicated by the no. 1) through Bregma −2.46 mm (indicated by the no. 6).

induction 0.21 versus 0.10 relative to respective control) (*SI Appendix*, Tables S3 and S4). Equally important, the cFos response in most brain regions was completely abolished by pretreatment with naloxone (Fig. 7*B* and *SI Appendix*, Table S4), including cerebral cortex, PFC, CPu, NAcc, septum, PVN, and lateral thalamus. These results suggest that the acute increase in food intake following activation of the Arc in Tg POMC-ChR2 mice is likely mediated by activation of the opioid receptor-signaling system with direct and indirect impact throughout the brain.

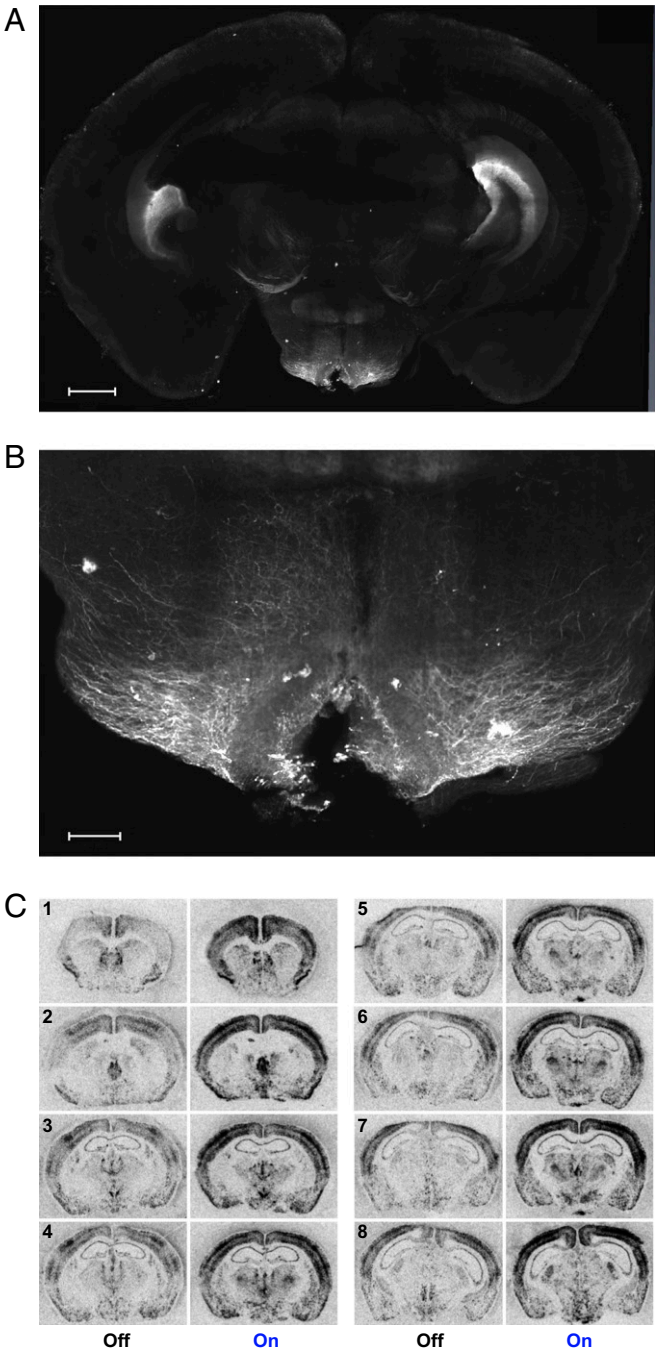

Fig. 6. Anatomical analysis of the projections of Arc neurons derived from POMC-expressing progenitors and the extent of activation in Tg POMC-ChR2 mice. (*A*) Labeled Arc neurons and their connectivity shown as a max intensity z-projection image. Representative image shows prominent arcuate connectivity with the dorsomedial, paraventricular, and lateral hypothalamus in the Tg POMC-ChR2 mouse brain slice (2-mm thickness) processed with the iDISCO method. (Scale bar, 1000 μm.) (*B*) Magnified view shows detailed eYFP expression pattern in the Arc. (Scale bar, 500 μm.) (*C*) ISH revealed cFos mRNA expression was intensively increased in broader brain areas in response to activation of Arc neurons of Tg POMC-ChR2 mice. Images were quantified with results shown in *SI Appendix*, Table S3. Representative images are shown ranging from Bregma 1.10 mm (indicated by the no. 1) through Bregma −2.12 mm (indicated by the no. 8).

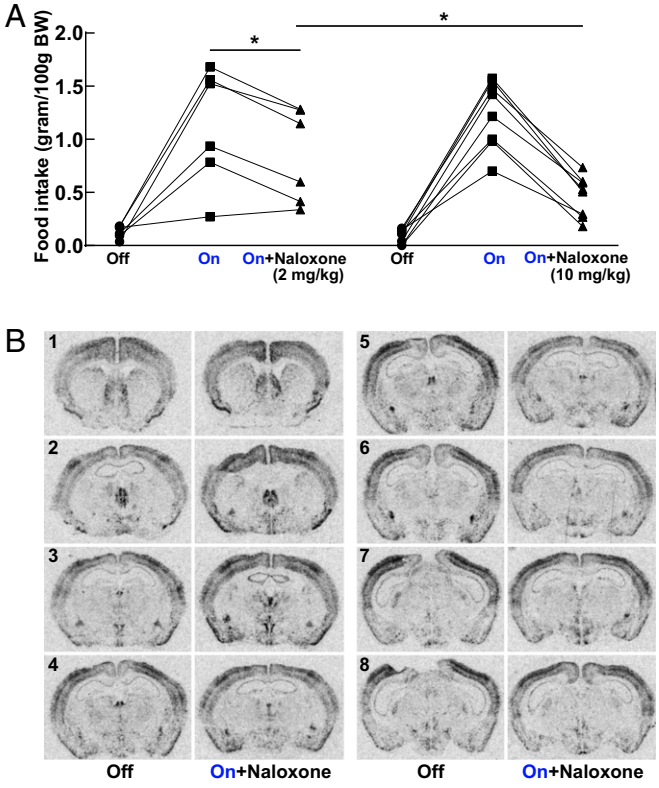

Fig. 7. Involvement of endogenous opioids in the increased feeding of Tg POMC-ChR2 mice. (*A*) Increased food intake in Tg POMC-ChR2 was reduced by pretreatment with naloxone in a dose-dependent manner ($n = 6$ mice in 2 mg/kg naloxone group; $n = 8$ mice in 10 mg/kg naloxone group). A multilevel regression model was used to assess the effects of light stimulation, naloxone treatment, and naloxone dosage on food intake, as well as a conditional effect of dosage on naloxone treatment (naloxone × dosage). Light stimulation increased food intake, $\beta = 1.08$, $T(25) = 12.26$, $P < 0.0001$, in a manner that was opposed by naloxone treatment at 2 mg/kg, $\beta = -0.33$, $T(25) = -2.61$, $^*P < 0.05$. The ability of naloxone to oppose the effects of the light stimulation was even stronger in the group of mice treated with a higher dosage of naloxone, $\beta = -0.42$, $T(25) = -2.71$, $^*P < 0.05$; 10 mg/kg versus 2 mg/kg. Otherwise food intake in these two groups of mice was similar, $\beta = 0.04$, $T(12) = 0.27$, $P = 0.79$. Mean ± SEM, 2 mg/kg naloxone group: 0.13 ± 0.02 (light off, saline); 1.13 ± 0.23 (light on, saline); 0.84 ± 0.18 (light on, naloxone); 10 mg/kg naloxone group: 0.092 ± 0.024 (light off, saline); 1.24 ± 0.11 (light on, saline); 0.46 ± 0.069 (light on, naloxone). (*B*) ISH revealed that cFos mRNA expression was either normalized or reduced in brain regions involved in reward and motivation by pretreatment with opioid antagonist naloxone (10 mg/kg). Images were quantified with results shown in *SI Appendix*, Table S4. Representative images are shown ranging from Bregma 1.10 mm (indicated by the no. 1) through Bregma −2.12 mm (indicated by the no. 8).

Discussion

In this study, we examined the relationship between cell-type–specific neuron activation and feeding behavior by optogenetic stimulation of both mature POMC neurons and neurons derived from POMC-expressing progenitors in the Arc of the hypothalamus. This body of work revealed the following main findings: (*i*) selective activation of POMC neurons rapidly inhibits feeding in food restricted animals; (*ii*) simultaneous activation of both POMC and orexigenic neurons derived from a common progenitor, including a subset of AgRP neurons, leads to a robust increase in feeding; (*iii*) 3D imaging delineates the projection pattern of adult hypothalamic POMC neurons versus the projection pattern of neurons derived from embryonic POMC-expressing cells that differentiate into POMC and a subset of the AgRP population; (*iv*) brain regions induced by activation of POMC alone and associated with reduced feeding include the cerebral cortex, lateral septum, PVN, dorsomedial hypothalamus, and the Arc; (*v*) coupling of neuronal activation and pharmacological treatment shows that activation of orexigenic neurons derived from POMC-expressing progenitors engages an extensive neural network that involves the endogenous opioid system. Thus, the increased food intake was blunted by pretreatment with naloxone, an opioid receptor antagonist. This was accompanied by the normalization of neural activity in most of the activated brain regions, including the cerebral cortex, PFC, CPu, NAcc, septum, PVN, and lateral thalamus.

In the Arc, posttranslational processing of the POMC prohormone results in two primary peptide products, α-MSH and β-endorphin (11). β-Endorphin is involved in pain regulation (12) and α-MSH mediates the anorexigenic effect on feeding (7, 25–29). In this study, both viral POMC-ChR2 and Tg POMC-ChR2 mice showed an analgesic effect induced by light stimulation, demonstrating functional activation of POMC neurons in these two animal models. Selective stimulation of POMC neurons in viral POMC-ChR2 mice led to decreased food intake, consistent with the observation that the hypothalamic melanocortin pathway is involved in feeding behavior (9, 10). This acute inhibition of feeding in fasted viral POMC-ChR2 mice is also consistent with pharmacological studies (25–29). Thus, an α-MSH agonist has a potent inhibitory effect on deprivation-induced food intake within 1 or 2 h (28, 29) when administrated in the PVN, a site that receives projections from Arc POMC neurons and where MC4-R expression is very high. However, our finding is in partial contrast with previous studies using optogenetic (30) or chemogenetic (31, 32) activation of POMC neurons. While these studies demonstrate reduced food consumption, they report that the effect is not evident until 24 h of stimulation in ad libitum-fed mice (30–32). One possibility for this discrepancy is that we used a different light-stimulation pattern in our study. Another difference is that our mice were fasted for 4 h, which may contribute to the more immediate effects of stimulation on feeding behavior. Our results suggest that Arc POMC neurons exert faster regulation of satiety in food-motivated mice. This finding is supported by a recent report that at least some Arc POMC neurons may act on faster time scales to reduce the drive to seek food (33). The combination of these pharmacological and opto- or chemogenetic studies would lead to a more complex view of the role of POMC in food regulation, whereby it would exert a long-term modulatory role based on metabolic status in the freely feeding animals, but is also active on shorter time scales during times when the animal is motivated to eat and the monitoring of food intake by these appetitive circuits is more critical. This does not preclude other mechanisms that recruit POMC to induce eating cessation (31, 32).

Surprisingly, in Tg POMC-ChR2 mice, activation of Arc neurons derived from POMC-expressing progenitors evoked voracious feeding. We have demonstrated that in these animals, ChR2 is expressed in both POMC- and AgRP-positive neurons, and these two groups of neurons are simultaneously activated as determined by cFos protein induction. The POMC neurons in the Arc were also functionally activated as evidenced by the pain regulation experiment in this animal model. The increased food intake in Tg POMC-ChR2 mice demonstrates that activation of this subset group of orexigenic neurons derived from POMC-expressing progenitors overrides the anorexigenic effect contributed by POMC neuron activation. It is well established that POMC and AgRP/NPY neurons in the Arc exert opposing actions on feeding to maintain energy homeostasis in the body (8, 14). Genetic and pharmacological evidence suggests that AgRP/NPY neurons promote feeding and increase body weight (8–10). Opto- or chemogenetic stimulation of AgRP neurons promotes intense food consumption (30, 34–36). The opposing effects on

food consumption following optogenetic activation in the transgenic and the viral models and their differences in potency stand in sharp contrast to the effects on analgesia. Thus, optogenetic stimulation in both the viral and the transgenic models produced comparable analgesic potency. This is likely because, in both cases, the analgesia is elicited from the activation of POMC neurons only, whereas the food regulation is the result of the relative power of POMC versus AgRP/NPY neurons. Taken together, our finding of increased food intake in Tg POMC-ChR2 mice suggests that mechanisms that increase satiety may not be as effective under conditions that enhance the inhibition of food consumption and oppose AgRP.

The increased food intake in Tg POMC-ChR2 mice can be largely blocked by pretreatment with the nonselective opioid receptor antagonist naloxone, suggesting involvement of the opioid receptor-signaling system. Other neural systems may also contribute to this increased food intake because naloxone did not completely block the increased food intake. Opioids are a family of peptides that differentially interact with three receptor classes (37). Anatomical studies have demonstrated that opioid receptors and peptides are widely distributed throughout the brain (38), including in a number of hypothalamic nuclei. Given the wide distribution of opioid receptors and the presence of other neuropeptides in the vicinity of opioidergic pathways, opioids are in position to affect many aspects of feeding and energy homeostasis (39, 40). Pharmacological studies have indicated that opioids stimulate food intake, whereas opioid antagonists are inhibitory (39, 40). It should be noted that this increased food intake in Tg POMC-ChR2 mice may not be solely due to the release of endogenous β-endorphin. Selective activation of POMC neurons in unsated viral POMC-ChR2 mice induced a reduction of food intake despite the possibility that endogenous β-endorphin was likely released as evidenced by an analgesic effect during the hot-plate test.

We then investigated the possible neural mechanisms whereby activation of Arc neurons derived from POMC-expressing progenitors led to increased food intake while selective activation of POMC neurons resulted in decreased food intake using cFos mRNA as a marker. Selective activation of POMC neurons in viral POMC-ChR2 mice led to neural activation in limited brain regions that are typically thought of as regulating food intake (41), including cerebral cortex, lateral septum, PVN, dorsomedial hypothalamus, and Arc. Classic lesion studies in PVN, dorsomedial, or ventromedial hypothalamus induced hyperphagia and obesity, while electrical stimulation increased food intake (6). In addition, we found increased neural activity in cerebral cortex and lateral septum following stimulation of Arc POMC neurons, indicating their possible involvement in regulating food intake.

In contrast, activation of the Arc in Tg POMC-ChR2 mice resulted in an intensive cFos response in broader areas of the brain thought to modulate feeding behavior (8, 42–44), including cerebral cortex, PFC, NAcc, septum, PVN, LH, and dorsomedial hypothalamus. More importantly, the neuronal activity in cerebral cortex, PFC, CPu, NAcc, septum, and PVN was normalized by pretreatment with naloxone, while the neuronal activity of the LH was reduced by 52% with the same pretreatment. Several of these responsive regions, such as the PFC, the NAcc, and the LH, have connections with reward systems and motivated behavior that modulate feeding (42–44). For example, activation of dopamine D1 receptor-expressing neurons in the PFC increases food intake (45). The NAcc functions as a major projection area for food reward and motivation in the mesolimbic dopaminergic system (42). The LH is known to be a critical neuroanatomical substrate for motivated feeding behavior in corticostriatal–hypothalamic circuitry (43). Thus, the activation of the subset of orexigenic neurons derived from POMC-expressing progenitors in Tg POMC-ChR2 mice may influence the rewarding characteristics of food and/or the motivational component of feeding.

We also investigated the architecture of neural circuits specifically originating from Arc peptidergic neurons on a brain-wide scale in these two animal models via 3D visualization. In the viral POMC-ChR2 mice, CLARITY processing showed that Arc POMC neurons project to a number of brain regions (*SI Appendix*, Table S1), consistent with previous anatomical studies (46, 47). Our detailed mapping of Arc POMC neuronal connectivity points to functional studies on the roles and circuit mechanisms underlying the regulation of feeding in these areas. The apparent diffuse projections of Arc POMC terminals observed suggest that POMC participates in the regulation of food consumption not only through hypothalamic structures, but also extrahypothalamic nuclei, including the amygdala, zona incerta, and lateral septum. More specifically, the amygdala is of interest as it is an area implicated in emotional aspects of feeding behavior. Recent studies have also shown that activation of zona incerta GABAergic neurons results in rapid binge-like eating behavior (48), while inactivation of lateral septum neurons blunts ventral hippocampus-induced suppression of feeding (49). However, it is still not fully understood how the inputs from Arc POMC neurons affect the neuronal physiology in these brain regions or their potential regulation of feeding behavior. In contrast to the viral POMC-ChR2 mice, a seemingly greater intensity of hypothalamic eYFP signal in the Tg POMC-ChR2 mice necessitated diminishing the comparatively less intense extrahypothalamic projections through the image threshold function. Nevertheless, the 3D visualization of neuronal projections in Tg POMC-ChR2 mice highlights the extensive neuronal communication between the Arc and lateral hypothalamic nucleus which is at the center of feeding control.

In sum, the POMC-expressing progenitors in the Arc differentiate into two functionally distinct neuronal subpopulations to influence feeding behavior in adulthood. Furthermore, the differences in food intake are associated with distinct projection and activation patterns of Arc neurons derived from POMC-expressing lineages compared with adult hypothalamic POMC neurons. Translational applications that aim to control appetite likely need to target the activation rather than the inhibition mechanisms and to modulate either the AgRP system itself or its downstream mediators. The fact that increased food intake in Tg POMC-ChR2 mice can be blunted by the opioid antagonist naloxone coupled with the normalization of neuronal activity in brain regions involved in reward and motivation highlights the potential value of targeting opioid receptor signaling to control feeding behavior.

Materials and Methods

Animals. POMC-Cre and Rosa26-CAG-stop^{flox}-ChR2(H134R)-eYFP (Ai32) mice were generated as previously described (16, 17). All experiments were conducted in accordance with the principles and procedures outlined in the National Institutes of Health Guidelines for the Care and Use of Animals and were approved by the Institutional Animal Care and Use Committee at the University of Michigan. More detailed information is provided in *SI Appendix, SI Material and Methods*.

Stereotactic Surgery and Virus Vector Injection. For the Tg POMC-ChR2 mice, optical fiber was unilaterally placed above the right Arc [coordinates, Bregma: (anterior–posterior, AP) −1.62 mm, (dorso–ventral, DV) 5.60 mm, (medio–lateral, ML) 0.33 mm]. For the POMC-Cre mice, Cre-dependent double-floxed deno-associated virus AAV5-EF1α-DIO-ChR2(H134R)-eYFP (50) was injected unilaterally in the right Arc [coordinates, Bregma: (AP) −1.62 mm, (DV) 5.70 mm, (ML) 0.30 mm]. Following injection, optical fiber was implanted over the Arc [(AP) −1.62 mm, (DV) 5.45 mm, (ML) 0.30 mm]. This mouse line of POMC-Cre with selectively expression of ChR2 in adulthood by viral-mediated method is referred to as viral POMC-ChR2. For details see *SI Appendix, SI Material and Methods*.

Slice Electrophysiology. For whole-cell current-clamp recordings, ChR2-eYFP-positive neurons in the Arc from acute slices were stimulated with repeated light-stimulation patterns used in the hot-plate and food intake tests of the current study. For details see *SI Appendix, SI Material and Methods*.

Immunohistochemistry. Staining of brain sections from viral POMC-ChR2 and Tg POMC-ChR2 mice with anti-GFP, anti-POMC, anti-AgRP, anti–β-endorphin, and anti-cFos was done as described in *SI Appendix, SI Material and Methods*. For all cFos protein induction experiments, mice received 6 min of blue laser (473 nm) stimulation (10 Hz, 15-ms pulses, 4.3 mW on the tip of fiber) in the open field chamber, then returned to their home cage. Animals were perfused 90 min after the onset of light stimulation. For details see *SI Appendix, SI Material and Methods*.

Behavioral Experiments. All behavioral tests were conducted at least 3-wk postsurgery during the same circadian period (0900–1600). Mice were handled and attached to the optical fiber without photostimulation for 4 d before behavioral tests. For the hot-plate test, the latency (in seconds) for the mice to lick their paws was measured (cutoff time, 60 s). On 3 consecutive testing days, mice were connected to the optical fiber and placed in an empty mouse cage for 5 min (day 1, blue laser off; day 2, blue laser on; day 3, blue laser off). Immediately following this 5-min period, mice were then tested on the hot plate. Blue laser stimulation (15-ms pulses, 10 Hz, 4.3 mW on the tip of fiber) on day 2 continued until the completion of the test. For naloxone pretreatment studies, mice were injected intraperitoneally with saline or naloxone HCl (10 mg/kg) 15 min before laser stimulation.

For the regular food intake test, mice had ad libitum access to standard laboratory pellet food in the home cage before and after tests. Each mouse was tested at the same time each day. Food consumption was measured for 30 min for 3 consecutive days (day 1, laser off; day 2, blue laser on; day 3, blue laser off). The laser stimulation parameters used on day 2 were 15-ms light pulses at 10 Hz for 30 s every minute for 30 min with 4.3 mW light power on the tip of fiber. For naloxone pretreatment in the Tg POMC-ChR2 mouse line, animals were injected intraperitoneally with saline or naloxone (2 mg/kg; 10 mg/kg) 15 min before laser stimulation. For the food intake test in viral POMC-ChR2 mice, animals were food deprived for 4 h with water freely available before the regular food intake test each day. The laser stimulation on day 2 was the same as described above. More detailed information is provided in *SI Appendix, SI Material and Methods*.

Three-Dimensional Visualization. For 3D imaging of immunofluorescence in viral POMC-ChR2 mice, the CLARITY procedure (19–21) was followed (*SI Appendix, SI Material and Methods*). For 3D imaging of immunofluorescence in Tg POMC-ChR2 mice, the iDISCO method (22) was followed (*SI Appendix, SI Material and Methods*). CLARITY optimized light sheet microscope (COLM) was used to acquire the images (20). Tiles of acquired image stacks were stitched together using TeraStitcher and subsequently visualized in 2D through orthoslice mode and in 3D through maximum intensity projection volume rendering mode using Amira 3D software.

cFos mRNA Expression Following Optogenetic Stimulation. For all cFos mRNA response experiments, mice received 6 min of either blue laser stimulation (10 Hz, 15-ms pulses, 4.3 mW on the tip of fiber) or no laser stimulation in the open field chamber, and then were returned to their home cage. Mice were killed by rapid decapitation 30 min after the onset of laser stimulation and their brains were dissected. For naloxone pretreatment in the Tg POMC-ChR2 mouse line, animals were injected intraperitoneally with naloxone (10 mg/kg) 15 min before laser stimulation. In situ hybridization (ISH) methodology was performed as previously described (51). For details see *SI Appendix, SI Material and Methods*.

Statistical Analysis. Statistical analyses were performed using Prism 7.0 (GraphPad) software or R software. $P < 0.05$ was considered statistically significant. Experimental animals demonstrating inaccurate viral injection or cannula sites were excluded from the present study since these subjects lacked expression of the reporter gene or neuronal activity marker cFos. These validation parameters were established before data analysis. For the naloxone pretreatment study on feeding behavior in Tg POMC-ChR2 mice, a multilevel regression model (also known as a hierarchical linear model or a mixed-effects model) was used to assess the effects of light, naloxone treatment, and naloxone dosage on food intake, while accounting for within-subjects design. These analyses were performed in R (R v.3.3.0: https://cran.r-project.org; RStudio v.0.99.896: www.rstudio.com/) using the *lme()* function in the *nlme* package (https://CRAN.R-project.org/package=nlme) with a default correlation structure (no within-group correlation) and method (restricted maximum likelihood). Our model included the fixed effects of the factors light (reference level = off), naloxone treatment (reference level = no naloxone), and dosage (reference level = 2 mg/kg), as well as a conditional effect of dosage on naloxone treatment (naloxone × dosage), with repeated measures accounted for by including individual subjects as a random effects variable (random intercept).

ACKNOWLEDGMENTS. We thank Drs. Megan Hagenauer and Aram Parsegian for help on statistical analysis; Dr. Cortney Turner for helpful discussion of the manuscript; and Limei Zhang and Hui Li for technical assistance. This work was supported by NIH Grants R01MH104261 and ONR N00014-12-1-0366, the Hope for Depression Research Foundation, and the Pritzker Neuropsychiatric Research Consortium.

1. Ogden CL, et al. (2006) Prevalence of overweight and obesity in the United States, 1999–2004. *JAMA* 295:1549–1555.
2. Olszewski PK, Levine AS (2007) Central opioids and consumption of sweet tastants: When reward outweighs homeostasis. *Physiol Behav* 91:506–512.
3. Sominsky L, Spencer SJ (2014) Eating behavior and stress: A pathway to obesity. *Front Psychol* 5:434.
4. Flier JS, Maratos-Flier E (1998) Obesity and the hypothalamus: Novel peptides for new pathways. *Cell* 92:437–440.
5. Elmquist JK, Elias CF, Saper CB (1999) From lesions to leptin: Hypothalamic control of food intake and body weight. *Neuron* 22:221–232.
6. Hoebel BG, Teitelbaum P (1962) Hypothalamic control of feeding and self-stimulation. *Science* 135:375–377.
7. Cone RD (2005) Anatomy and regulation of the central melanocortin system. *Nat Neurosci* 8:571–578.
8. Morton GJ, Meek TH, Schwartz MW (2014) Neurobiology of food intake in health and disease. *Nat Rev Neurosci* 15:367–378.
9. Ollmann MM, et al. (1997) Antagonism of central melanocortin receptors in vitro and in vivo by agouti-related protein. *Science* 278:135–138.
10. Cowley MA, et al. (1999) Integration of NPY, AGRP, and melanocortin signals in the hypothalamic paraventricular nucleus: Evidence of a cellular basis for the adipostat. *Neuron* 24:155–163.
11. Akil H, Watson SJ (1980) Neuromodulatory functions of the brain pro-opiocortin system. *Adv Biochem Psychopharmacol* 22:435–445.
12. Loh HH, Tseng LF, Wei E, Li CH (1976) beta-endorphin is a potent analgesic agent. *Proc Natl Acad Sci USA* 73:2895–2898.
13. Millington GWM (2007) The role of proopiomelanocortin (POMC) neurones in feeding behaviour. *Nutr Metab (Lond)* 4:18.
14. Schwartz MW, Porte D, Jr (2005) Diabetes, obesity, and the brain. *Science* 307:375–379.
15. Padilla SL, Carmody JS, Zeltser LM (2010) Pomc-expressing progenitors give rise to antagonistic neuronal populations in hypothalamic feeding circuits. *Nat Med* 16:403–405.
16. McHugh TJ, et al. (2007) Dentate gyrus NMDA receptors mediate rapid pattern separation in the hippocampal network. *Science* 317:94–99.
17. Madisen L, et al. (2012) A toolbox of Cre-dependent optogenetic transgenic mice for light-induced activation and silencing. *Nat Neurosci* 15:793–802.
18. Akil H, Young E, Walker JM, Watson SJ (1986) The many possible roles of opioids and related peptides in stress-induced analgesia. *Ann N Y Acad Sci* 467:140–153.
19. Chung K, Deisseroth K (2013) CLARITY for mapping the nervous system. *Nat Methods* 10:508–513.
20. Tomer R, Ye L, Hsueh B, Deisseroth K (2014) Advanced CLARITY for rapid and high-resolution imaging of intact tissues. *Nat Protoc* 9:1682–1697.
21. Yang B, et al. (2014) Single-cell phenotyping within transparent intact tissue through whole-body clearing. *Cell* 158:945–958.
22. Renier N, et al. (2014) iDISCO: A simple, rapid method to immunolabel large tissue samples for volume imaging. *Cell* 159:896–910.
23. Anderson EJ, et al. (2016) 60 YEARS OF POMC: Regulation of feeding and energy homeostasis by α-MSH. *J Mol Endocrinol* 56:T157–T174.
24. Overstreet LS, et al. (2004) A transgenic marker for newly born granule cells in dentate gyrus. *J Neurosci* 24:3251–3259.
25. Fan W, Boston BA, Kesterson RA, Hruby VJ, Cone RD (1997) Role of melanocortinergic neurons in feeding and the agouti obesity syndrome. *Nature* 385:165–168.
26. Rossi M, et al. (1998) A C-terminal fragment of Agouti-related protein increases feeding and antagonizes the effect of alpha-melanocyte stimulating hormone in vivo. *Endocrinology* 139:4428–4431.
27. Nakazato M, et al. (2001) A role for ghrelin in the central regulation of feeding. *Nature* 409:194–198.
28. Giraudo SQ, Billington CJ, Levine AS (1998) Feeding effects of hypothalamic injection of melanocortin 4 receptor ligands. *Brain Res* 809:302–306.
29. Cowley MA, et al. (2001) Leptin activates anorexigenic POMC neurons through a neural network in the arcuate nucleus. *Nature* 411:480–484.
30. Aponte Y, Atasoy D, Sternson SM (2011) AGRP neurons are sufficient to orchestrate feeding behavior rapidly and without training. *Nat Neurosci* 14:351–355.
31. Zhan C, et al. (2013) Acute and long-term suppression of feeding behavior by POMC neurons in the brainstem and hypothalamus, respectively. *J Neurosci* 33:3624–3632.

32. Fenselau H, et al. (2017) A rapidly acting glutamatergic ARC→PVH satiety circuit postsynaptically regulated by α-MSH. *Nat Neurosci* 20:42–51.
33. Mandelblat-Cerf Y, et al. (2015) Arcuate hypothalamic AgRP and putative POMC neurons show opposite changes in spiking across multiple timescales. *eLife* 4:07122.
34. Krashes MJ, et al. (2011) Rapid, reversible activation of AgRP neurons drives feeding behavior in mice. *J Clin Invest* 121:1424–1428.
35. Atasoy D, Betley JN, Su HH, Sternson SM (2012) Deconstruction of a neural circuit for hunger. *Nature* 488:172–177.
36. Chen Y, Lin YC, Zimmerman CA, Essner RA, Knight ZA (2016) Hunger neurons drive feeding through a sustained, positive reinforcement signal. *eLife* 5:18640.
37. Akil H, et al. (1984) Endogenous opioids: Biology and function. *Annu Rev Neurosci* 7: 223–255.
38. Mansour A, Fox CA, Akil H, Watson SJ (1995) Opioid-receptor mRNA expression in the rat CNS: Anatomical and functional implications. *Trends Neurosci* 18:22–29.
39. Kalra SP, Horvath TL (1998) Neuroendocrine interactions between galanin, opioids, and neuropeptide Y in the control of reproduction and appetite. *Ann N Y Acad Sci* 863:236–240.
40. Glass MJ, Billington CJ, Levine AS (1999) Opioids and food intake: Distributed functional neural pathways? *Neuropeptides* 33:360–368.
41. Gao Q, Horvath TL (2007) Neurobiology of feeding and energy expenditure. *Annu Rev Neurosci* 30:367–398.
42. Kelley AE, Baldo BA, Pratt WE, Will MJ (2005) Corticostriatal-hypothalamic circuitry and food motivation: Integration of energy, action and reward. *Physiol Behav* 86: 773–795.
43. Stuber GD, Wise RA (2016) Lateral hypothalamic circuits for feeding and reward. *Nat Neurosci* 19:198–205.
44. Saper CB, Chou TC, Elmquist JK (2002) The need to feed: Homeostatic and hedonic control of eating. *Neuron* 36:199–211.
45. Land BB, et al. (2014) Medial prefrontal D1 dopamine neurons control food intake. *Nat Neurosci* 17:248–253.
46. Bagnol D, et al. (1999) Anatomy of an endogenous antagonist: Relationship between Agouti-related protein and proopiomelanocortin in brain. *J Neurosci* 19:RC26.
47. Wang D, et al. (2015) Whole-brain mapping of the direct inputs and axonal projections of POMC and AgRP neurons. *Front Neuroanat* 9:40.
48. Zhang X, van den Pol AN (2017) Rapid binge-like eating and body weight gain driven by zona incerta GABA neuron activation. *Science* 356:853–859.
49. Sweeney P, Yang Y (2015) An excitatory ventral hippocampus to lateral septum circuit that suppresses feeding. *Nat Commun* 6:10188.
50. Tsai HC, et al. (2009) Phasic firing in dopaminergic neurons is sufficient for behavioral conditioning. *Science* 324:1080–1084.
51. Aurbach EL, et al. (2015) Fibroblast growth factor 9 is a novel modulator of negative affect. *Proc Natl Acad Sci USA* 112:11953–11958.